

© The Author 2009. Published by Oxford University Press. All rights reserved. For Permissions, please email: journals.permissions@oxfordjournals.org

Multi-directional tumor suppressive activity of AIMP2/p38 and the enhanced susceptibility of AIMP2 heterozygous mice to carcinogenesis.

Jin Woo Choi¹, Jung Yeon Um¹, Joydeb Kumar Kundu², Young-Joon Surh² and Sunghoon Kim^{1,3*}

¹Center for Medicinal Protein Network and Systems Biology, ²National Research Laboratory of Molecular Carcinogenesis and Chemoprevention, WCU Department of Molecular Medicine and Biopharmaceutical Sciences, College of Pharmacy, Seoul National University, Seoul 151-742, Korea

³Integrated Bioscience and Biotechnology Institute, Advanced Institutes of Convergence Technology, Seoul National University, Suwon 443-270, Korea

*To whom correspondence should be addressed. Tel: +82 2 880 8180; Fax: +82 2 875 2621;

E-mail: sungkim@snu.ac.kr

Abstract

AIMP2 is a factor associated with the macromolecular protein synthesis machinery consisting of nine different aminoacyl-tRNA synthetases and three non-enzymatic factors. However, it was shown to work as a multi-faceted regulator through the versatile interactions with diverse signal mediators. For instance, it can mediate pro-apoptotic response to DNA damage and TNF- α stimulus and growth-arresting signal by TGF- β . Considering that these pathways are critically implicated in the control of tumorigenesis, AIMP2 is expected to work as a potent tumor suppressor with broad coverage against different cancer types. Here we investigated whether AIMP2 would give gene dosage effect on its pro-apoptotic and anti-proliferative activities using the wild type, hetero- and homozygous AIMP2 cells and whether AIMP2 would be critical in preventing tumorigenesis using different *in vivo* tumor models. Both the apoptotic responses to DNA damage and TNF- α and sensitivity to growth arresting TGF- β signal were reduced in AIMP2 hetero- and homozygous cells compared with the wild type cells in dose-dependent manner. In all of the *in vivo* carcinogenesis experiments, reduction of AIMP2 level in heterozygous AIMP2 mice provided higher susceptibility to tumor formation. Thus, this work proves the functional significance of AIMP2 in determination of cell proliferation and death, and as a haploinsufficient tumor suppressor.

Abbreviations : ARS, aminoacyl-tRNA synthetases; AIMP, ARS- interacting multifunctional protein; MEF, mouse embryonic fibroblast; BPDE, anti-benzo[*a*]pyrene-7,8-dihydrodiol-

9,10-epoxide; B[a]P, Benzo[a]pyrene; DMBA, dimethylbenz[a]anthracene; TPA, 12-*O*-tetradecanoylphorbol-13- acetate; AOM, azoxymethane; DSS, dextran sulfate sodium

Introduction

Mammalian aminoacyl-tRNA synthetases (ARSs) form macromolecular protein complex with intriguing structure and function [1,2]. This complex consists of nine different ARSs and three non-enzymatic factors called AIMP1, 2 and 3 which are also known as p43, p38 and p18, respectively. While the multi-ARS complex is in charge of protein synthesis, its components are functionally involved in diverse regulatory pathways and human diseases [3]. Among them, AIMP3/p18 was previously shown to be a haploinsufficient tumor suppressor, playing a critical role in the maintenance of chromosome integrity [4]. Although AIMP2/p38 plays a scaffolding role in the assembly of the whole complex [5], it also controls major signaling pathways that are critically involved in cell death and proliferation. For instance, AIMP2 mediates pro-apoptotic activity via p53 in response to DNA damage [6]. Recently, we demonstrated that AIMP2 promotes ubiquitin-mediated degradation of TRAF2, an important regulator of TNF- α signal pathway, enhancing apoptotic response of the cells to TNF- α [7]. In addition, it arbitrates anti-proliferative activity of TGF- β through the down-regulation of c-MYC [8]. Considering its comprehensive coverage in these signaling pathways that are significantly implicated in various cancers, any disruption of AIMP2 activity and expression is expected to give significant impact on cell fate. In this work, we examined the gene dosage effect of AIMP2 on DNA damage- or TNF- α -induced cell death and on TGF- β -induced growth arrest. We also investigated whether reduced expression of AIMP2 would actually elevate tumor susceptibility using a few different *in vivo* carcinogenesis models.

Materials and Methods

Cell culture

Embryonic 12.5d AIMP2^{+/+}, AIMP2^{+/-} and AIMP2^{-/-} MEFs were established in DMEM

(Hyclone) containing 10% fetal bovine serum and 2% penicillin and streptomycin. The cells from passage numbers 2 to 5 were used for experiments. To test cell death by anti-benzo[*a*]pyrene-7,8-dihydrodiol-9,10-epoxide (BPDE, from NCI Chemical Repository), each group of the MEF cells were cultured on 10 plates (35mm) and treated with BPDE (0.1 μ M), and the numbers of the live cells in the two selected plates were counted in two day intervals. To test growth inhibition by TGF- β , the MEF cells were cultivated in the presence or absence of TGF- β , and sub-cultured in two day intervals.

Flow cytometry

Embryonic 12.5 day AIMP2^{+/+}, AIMP2^{+/-} and AIMP2^{-/-} MEF cells were cultivated in the absence or presence of cycloheximide (10 μ g/ml) and TNF- α (30ng/ml) for 16 h, then fixed in 70% ethanol for 1 h at 4°C and washed with ice-cold PBS twice. Following this, 1x10⁶ cells were stained with propidium iodide (50 μ g/ml) containing 0.1% sodium citrate, 0.3% NP40 and 50 μ g/ml RNase A and left it standing for 40 min. Samples then were subjected to flow cytometry (FACS Calibur, Beckton-Dickinson) for the determination of apoptotic cells by counting sub-G1 cells and Annexin V staining following the manufacturer's instruction (Invitrogen). For each sample, 20,000 cells were analyzed using Cell Quest Pro software. All of the experiments were repeated three times. For the analysis of cell death by DNA damage, the MEF cells were incubated for 16 h after exposure to UV (50J/m²).

Cell cycle arrest

1x10⁴ MEF cells were seeded on 12 well plates. After changing with serum-free media, the cells were treated with TGF- β (3ng/ml) for 18 h and 1 μ Ci [³H] thymidine was added to each well for 6 h. The cells were washed with cold PBS and precipitated with 10% cold TCA.

Radioactivity of the lysates was measured by scintillation counter. The inhibition percentage of cell cycle was calculated using the following formula:

$$100 - \left[\frac{\text{radioactivity of the cell lysate in the presence of TGF-}\beta}{\text{radioactivity of the cell lysate in the absence of TGF-}\beta} \right] \times 100$$

Reporter assay

To test the NF- κ B-dependent transcriptional activity, NF- κ B-luciferase vector (kindly provided by Dr. Jonathan Ashwell, NIH) was transfected into MEFs using Lipofectamine (Invitrogen). After 24 h, TNF- α was added to cells for 16 h. The cell lysates were prepared and reacted for luciferase activity using the assay kit and following the manufacturer's protocol (Promega) and the activity was quantified by luminometer. We also monitored the effect of MYC on the target genetic expression using the cyclin D1-dependent luciferase system (a kind gift from Dr. Sung Hee Baek, Seoul National University).

Immunoblot analysis

The MEFs were harvested 2 h after exposure to UV (50 J/m²) and lysed in the 50mM Tris-HCl buffer (pH 7.5) containing 1% Triton X 100 and 0.1% SDS. Anti-p53 (FL-393) and -p21 (H-164) antibodies were purchased from Santa Cruz and phospho-p53 (ser15) antibody was from Cell Signaling. Anti-AIMP2 (#324) monoclonal antibody was purchased from Neomics (Korea). For analysis of TNF- α signaling, TNF- α was treated for the indicated times, and I κ B level was determined using Western blotting with anti-I κ B antibody (Cell Signaling).

Two-stage skin papillomagenesis

Wild type (n=12) and heterozygous (n=11) AIMP2 mice were treated on their shaven backs

with a single topical dose of dimethylbenz[*a*]anthracene (DMBA, 0.2 μ mol, Sigma) dissolved in 0.2ml acetone:DMSO (85:15 v/v) or the same volume of solvent alone. One week after initiation with DMBA, 12-*O*-tetradecanoylphorbol-13-acetate (TPA, 10nmol / 0.2ml acetone, Sigma) was topically applied to the animals twice a week until termination of the experiments. Starting 1 week after the promoter treatment, tumors of at least 1 mm diameter were counted in intervals of a week for 20 weeks. The results were expressed as the percentage of mice bearing papilloma or carcinoma (incidence) and the average number of papillomas or carcinoma per mouse (multiplicity).

Lung carcinogenesis study

Benzo[*a*]pyrene (BP, 100mg/kg body weight, Sigma) was intraperitoneally injected into 6 week old outbred C57BL/6 mice, once a week for two weeks. BP was dissolved in 0.9% saline containing 35% PEG400 and 10% DMSO. To check tumor formation, the mice were randomly sacrificed at time interval from 6 weeks after injection.

Two-stage colon carcinogenesis

To test the physiologic relevance of AIMP2 expression in colitis-associated to colon cancer in vivo, we used azoxymethane (AOM)/dextran sulfate sodium (DSS)-induced colon cancer model. AIMP2^{+/+} and AIMP2^{+/-} C57/BL6 mice were injected intraperitoneally (i.p.) with 15 mg/kg AOM (Sigma). After 7 days, 2% DSS (MP Biochemicals, Irvine, CA) was given in their drinking water over 5 days, followed by 16 days of regular water. This cycle was repeated 3 times and mice were sacrificed 9 days after the last cycle.

Histopathology

The target tissues (papilloma, lung and colon) were isolated, flushed with PBS, fixed in 10%

formalin for 24 h. The tissues were then processed to a paraffin block. After deparaffinization and hydration, the tissue slides were stained by hematoxylin and eosin. Immunohistochemistry staining was accomplished as following. For antigen retrieval was accomplished by incubating with 0.3% H₂O₂ and then boiling in 0.01M citrate buffer. After blocking with 4% BSA, the antibodies against PCNA (FL-261) and cyclin D1 (H-295) from Santacruz were added for 2 h. And then polymer kit (Dako) and diaminobenzidine (Dako) were used for staining following the manufacturer's instruction. The stained specimen was subjected to be examined by a professional pathologist.

TUNNEL staining

To detect apoptosis in tissues, we used apoptag kit (Chemicon) following the manufacturer's instruction. Briefly, after deparaffinizing the sections and digesting proteins with proteinase K, the slides were incubated in the equilibration buffer containing TdT enzyme, followed by stop/wash buffer. Then 50µl of anti-digoxigenin-fluorescein was added and the slides were covered with mounting solution containing 0.5µg/ml propidium iodine.

Quantitative RT-PCR

The transcript levels of murine c-MYC (target) and β-actin (endogenous reference) were determined by quantitative real time RT-PCR. Total RNAs from the MEFs were isolated using Trizol (Invitrogen) and converted to cDNAs by Moloney murine leukemia virus reverse transcriptase (Invitrogen) and random hexmer set. All PCR reactions were performed with SYBR green master mix kit (Roche) and in Roche LightCycler 2.0. The pairs of ATGCCCTCAACGTGAACTTC (forward) and CGCAACATAGGATGGAGAGCA (reverse) were used as the specific primers for c-MYC gene, and GGCTGTATTCCCCTCCATCG and CCAGTTGGTAACAATGCCATGT primers were for β-actin

Results

Differential apoptotic responses to DNA damage of MEFs with different AIMP2 genotype

Here we prepared mouse embryonic fibroblasts (MEFs) from the wild type (+/+), hetero- (+/-) and homozygous (-/-) AIMP2 mice and investigated whether they would show differential apoptotic responses to DNA damage depending on the genetic dosage of AIMP2. The cells were subjected to UV irradiation and the resulting apoptosis was monitored by sub-G1 phase cells using flow cytometry. While the sub-G1 phase cells were increased to about 20% in the wild type cells, heterozygous and homozygous AIMP2 cells generated about 12% and 7% level of sub-G1 cells, respectively (Figure 1A). DNA damage was also introduced by anti-benzo[*a*]pyrene-7,8-dihydrodiol-9,10-epoxide (BPDE) and the apoptotic response was determined by viable cell counting. Although the viable cells were almost undetectable from the wild type cells after 8 days, about 32% and 40% of the hetero- and homozygous AIMP2 cells respectively were still viable under the same condition (Figure 1B). In the viable cell counting, hetero- and homozygous AIMP2 cells showed little difference, perhaps due to lower sensitivity of the assay. Since AIMP2 mediates apoptotic response via the activation of p53, we compared the response of p53 to UV irradiation between the three cells. UV-induced p53 phosphorylation also showed dependency on the copy number of AIMP2 gene (Figure 1C).

Effect of AIMP2 on the responses to TNF- α -induced cell death and NF- κ B activation

We also induced cell death by the treatment of TNF- α with cycloheximide and monitored apoptotic response by flow cytometry as above. The sub-G1 portion of the wild type, hetero- and homozygous AIMP2 cells increased to about 39%, 27% and 17%, respectively (Figure

2A). Since TNF- α -induced cell death is negatively influenced by the induction of NF- κ B, we also compared the TNF- α -dependent induction of NF- κ B using luciferase assay system that is controlled by NF- κ B. The TNF- α -dependent increase of luciferase activity was most prominent in the AIMP2^{-/-} cells and then reduced in the order of AIMP2^{+/-} and AIMP2^{+/+} cells (Figure 2B). We also compared the effect of AIMP2 on the reduction of I κ B that hold NF- κ B in the cytoplasm. Upon treatment with TNF- α , I κ B is phosphorylated and degraded, releasing NF- κ B for nuclear localization. I κ B level of AIMP2^{-/-} cells were most significantly reduced in 15 min after treatment with TNF- α . However, I κ B level of AIMP2^{+/-} cells reached the minimal level in 30 min and it was only slightly reduced in the AIMP2^{+/+} cell by TNF- α treatment (Figure 2C). Thus, TNF- α -dependent apoptotic response also showed dosage dependency on AIMP2-encoding gene.

Differential sensitivity to anti-proliferative TGF- β signal

We previously reported that AIMP2 mediates growth-arresting signal of TGF- β via down regulation of c-MYC [8]. AIMP2^{+/+}, AIMP2^{+/-} and AIMP2^{-/-} cells were compared for their sensitivity to anti-proliferative activity of TGF- β by measuring [³H] thymidine incorporation. The proliferation of the wild type, hetero- and homozygous cells were reduced to about 20%, 8.5% and 1%, respectively, by the treatment of TGF- β (Figure 3A). We then compared whether the three MEFs would show different response to TGF- β signal in c-MYC expression. The expression of c-MYC was also monitored quantitatively by real time PCR of its transcript. Both in the presence and absence of TGF- β signal, c-MYC was expressed at the highest level in AIMP2^{-/-} cells and also in AIMP2^{+/-} and AIMP2^{-/-} cells (Figure 3B) in respective order. In additional assay, we compared the expression of c-MYC by monitoring

the expression of its target such as cyclin D1. We introduced the plasmid expressing cyclin D1-dependent luciferase into MEFs of three different genotypes and monitored luciferase activity. The luciferase activity was highest in AIMP2^{-/-} cells both in the absence and presence of TGF- β (Figure 3C). The cell growth in the absence and presence of TGF- β was compared by direct cell counting. Although cell growth of the wild type was reduced in the presence of TGF- β signal, only slight and little reduction in cell number were observed in the heterozygous and homozygous cells, respectively (Figure 3D). Combined together, AIMP2 is a multi-faceted cell regulator, mediating DNA damage- and TNF- α -induced cell death and TGF- β -dependent growth arrest (Figure 3E).

AIMP2 heterozygosity increases tumor susceptibility in two-stage skin papillomagenesis

Considering the broad coverage of AIMP2 in the determination of cell death and proliferation, it is expected to be a potent tumor suppressor. Here we examined this possibility using different *in vivo* carcinogenesis models. Since homozygous AIMP2 mice were neo-natal lethal [8], only the wild type and heterozygous mice could be used for the experiment. The skin cells were isolated from two different wild type and heterozygous AIMP2 mice and AIMP2 levels were compared by Western blotting. The heterozygous cells expressed AIMP2 at lower concentration as expected (Figure 4A). We first conducted two stage skin carcinogenesis experiment using dimethylbenz[*a*]anthracene (DMBA) and 12-*O*-tetradecanoylphorbol-13- acetate (TPA), which are representative carcinogen pairs inducing papilloma in skin [9]. The percentage of tumor-generating mice and the number of the tumors per mouse were determined at time interval after the chemical treatment. The heterozygous mice showed significantly higher incidence in tumor formation with earlier onset time (Figure 4B) and higher tumor number compared with those of the wild type (Figure 4C and

D). The papilloma were isolated and confirmed by histological examination (Figure 4E). We then examined apoptotic status in situ of the isolated papilloma by TUNNEL assay. The apoptotic signal was significantly reduced in the AIMP2 heterozygous papilloma (Figure 4F). We also compared the cell proliferation between the wild type and heterozygous papilloma by immunohistochemistry using PCNA and cyclinD1 as proliferation markers. Both markers showed higher staining intensity in the heterozygous tissues, suggesting higher proliferation status in AIMP2-reduced tissues (Figure 4G).

Enhanced tumor susceptibility of AIMP2 heterozygous mice to lung carcinogenesis

We also conducted lung carcinogenesis experiments using a carcinogen, benzo[*a*]pyrene (BP) treatment [10]. The expression of AIMP2 was also lower in AIMP2^{+/-} lung cells compared to that of the wild type cells (Figure 5A). We introduced BP by intraperitoneal injection as previously described [11] and compared the frequency of the tumor formation. AIMP2^{+/-} mice developed lung tumors at about 2 fold higher frequency than the wild type littermates (Figure 5B) and the tumor formation was also confirmed by histological examination of lungs (Figure 5C arrows).

Enhanced tumor susceptibility of AIMP2 heterozygous mice to two-stage colon carcinogenesis

After confirming lower expression of AIMP2 in AIMP2^{+/-} colon cells (Figure 6A), we induced colon cancer using azoxymethane (AOM) and dextran sulfate sodium (DSS), and the numbers of tumor nodules in colon and tumor sizes were compared. While the wild type mice generated about 5 tumors per mouse, the heterozygous mice generated about 8 tumors per mouse (Figure 6B) and the sizes of tumors in AIMP2^{+/-} mice were generally larger compared with those of the wild type mice (Figure 6C). Combined together, AIMP2 heterozygous mice

showed higher susceptibility to all of the tested carcinogenesis models, confirming the potential of AIMP2 as haploinsufficient tumor suppressor.

Discussion

Since cell proliferation and death are finely controlled through complex interactions amongst diverse cell regulators, disruption of their interplay can result in cancer formation. The impact of these factors on the determination of cell fate appears to be correlated with the number of signal pathways to which each factor is functionally linked [12] since abnormal expression or activity of these factors could widely affect the integrity of cellular regulatory network. Here we demonstrated that AIMP2 can function as a molecular hub regulating cell proliferation and death via the control of multiple signaling pathways.

Among components of three signaling pathways studied in this work, p53 is a well known tumor suppressor associated with different cancer types [13], and NF- κ B, a key factor of TNF- α pathway and c-MYC, a target factor down regulated by TGF- β are also implicated in diverse cancers [14-17]. In this work, we have employed three different carcinogenesis models to assess *in vivo* significance of AIMP2 as tumor suppressor. In human skin carcinoma, p53 and c-MYC appear to be critically implicated. However, the role of NF- κ B activity in this model is not excluded [18,19] although the exact role is not clear yet [20]. In cases of the human non-small cell lung cancer, which is mimicked by BP-induced tumor in mouse, aberrant activity and expression of p53 is most frequently observed and NF- κ B is also highly activated [21]. MYC over-expression is also reported in small cell lung cancer [22]. In colitis-related colon cancer, loss of heterozygosity or other mutation of p53 appears to be involved at primary stage of carcinogenesis [23-25]. Alterations in MYC expression and TGF- β signaling have also been reported from animal experiments and experiments

involving human patients [26, 27]. Highly activated NF- κ B appears to be significant in inflammation-associated colon cancer [15]. Although we cannot exactly deconvolute the influence of AIMP2 in each of these pathways, the increased susceptibility to tumorigenesis observed in AIMP2 heterozygous mice may have resulted from the combination of its multi-directional activities.

At this moment, we do not know how AIMP2, normally sequestered within a macromolecular protein complex in cytosol, can be involved in different signal pathways. In the case of its apoptotic interaction with p53 in response to DNA damage, phosphorylation of AIMP2 appears to be responsible for its dissociation from the complex and nuclear translocation for the interaction with p53 [6]. Considering this, it is also plausible that differential post-translational modification of AIMP2 may guide it to different target molecules. AIMP2 also seems to give contrasting effect on the cellular level of its target factors. For instance, it reduces FBP [8] and TRAF2 level [7] by mediating delivery of ubiquitin to these target factors whereas it enhances p53 level by blocking MDM2, the E3 ubiquitin ligase [6]. Despite its contrasting effect on target stability, it involves ubiquitin as a common factor, implying that there might be a general working mechanism of AIMP2 in the ubiquitin delivery system, which needs further investigation.

It is somewhat counter-intuitive that AIMP2 works as a tumor suppressor considering that it is physically associated with the multi-ARS complex. Since this complex contains many ARSs, the essential enzymes for protein synthesis, and AIMP2 is important for cellular stability of these enzymes [5], any defect of this factor is expected to cause a problem in protein synthesis, which may reduce cell proliferation. However, the cells deficient in AIMP2 showed increased cell proliferation and cellular protein synthesis was not significantly affected at least in culture condition with complete medium [5]. This fact implies that the function of AIMP2 as signal mediator could be more direct culprit. Among the three non-

enzymatic factors associated with the multi-ARS complex, AIMP1 was already shown to work as anti-cancer therapeutic protein with immune-stimulating and angiostatic cytokine activity [28-31]. In addition, mutations and allelic deletion of AIMP3 have been reported in cancer patients [29]. Here we report AIMP2 as another tumor suppressor with distinct activity and suggest its potential as a therapeutic target for anticancer agents.

Acknowledgements

This work was supported by the grants from the Acceleration Research of KOSEF (2009-0063498), the 21st Frontier Functional Proteomics Research (FPR0881-250) and R31-2008-000-10103-0 from the WCU project of the MEST and the KOSEF. We thank Drs. Jonathan Ashwell and Sung Hee Baek for materials.

Reference

1. Han, J.M., Lee, M.J., Park, S.G., Lee, S.H., Razin, E., Choi, E.C. and Kim, S. (2006) Hierarchical network between the components of the multi-tRNA synthetase complex: implications for complex formation. *J Biol Chem*, **281**, 38663-38667.
2. Lee, S.W., Cho, B.H., Park, S.G. and Kim, S. (2004) Aminoacyl-tRNA synthetase complexes: beyond translation. *J Cell Sci*, **117**, 3725-3734.
3. Park, S.G., Schimmel, P. and Kim, S. (2008) Aminoacyl tRNA synthetases and their connections to disease. *Proc Natl Acad Sci U S A*, **105**, 11043-11049.
4. Park, B.J., Kang, J.W., Lee, S.W., Choi, S.J., Shin, Y.K., Ahn, Y.H., Choi, Y.H., Choi, D., Lee, K.S. and Kim, S. (2005) The haploinsufficient tumor suppressor p18 upregulates p53 via interactions with ATM/ATR. *Cell*, **120**, 209-221.
5. Kim, J.Y., Kang, Y.S., Lee, J.W., Kim, H.J., Ahn, Y.H., Park, H., Ko, Y.G. and Kim, S.

- (2002) p38 is essential for the assembly and stability of macromolecular tRNA synthetase complex: implications for its physiological significance. *Proc Natl Acad Sci U S A*, **99**, 7912-7916.
6. Han, J.M., Park, B.J., Park, S.G., Oh, Y.S., Choi, S.J., Lee, S.W., Hwang, S.K., Chang, S.H., Cho, M.H. and Kim, S. (2008) AIMP2/p38, the scaffold for the multi-tRNA synthetase complex, responds to genotoxic stresses via p53. *Proc Natl Acad Sci U S A*, **105**, 11206-11211.
 7. Choi, J.W., Kim, D.G., Park, M. C., Um, J. Y., Han, J.M., Park, S. G., Choi, E.C. and Kim,S. (2009) AIMP2/p38 promotes TNF- α -dependent apoptosis via ubiquitin-mediated degradation of TRAF2. *J Cell Sci*, in press.
 8. Kim, M.J., Park, B.J., Kang, Y.S., Kim, H.J., Park, J.H., Kang, J.W., Lee, S.W., Han, J.M., Lee, H.W. and Kim, S. (2003) Downregulation of FUSE-binding protein and c-myc by tRNA synthetase cofactor p38 is required for lung cell differentiation. *Nat Genet*, **34**, 330-336.
 9. Stenback, F. (1980) Skin carcinogenesis as a model system: observations on species, strain and tissue sensitivity to 7,12-dimethylbenz(a)anthracene with or without promotion from croton oil. *Acta Pharmacol Toxicol (Copenh)*, **46**, 89-97.
 10. Boysen, G. and Hecht, S.S. (2003) Analysis of DNA and protein adducts of benzo[a]pyrene in human tissues using structure-specific methods. *Mutat Res*, **543**, 17-30.
 11. Wang, Y., Zhang, Z., Kastens, E., Lubet, R.A. and You, M. (2003) Mice with alterations in both p53 and Ink4a/Arf display a striking increase in lung tumor multiplicity and progression: differential chemopreventive effect of budesonide in wild-type and mutant A/J mice. *Cancer Res*, **63**, 4389-4395.
 12. Barabasi, A.L. and Oltvai, Z.N. (2004) Network biology: understanding the cell's

- functional organization. *Nat Rev Genet*, **5**, 101-113.
13. Whibley, C., Pharoah, P.D. and Hollstein, M. (2009) p53 polymorphisms: cancer implications. *Nat Rev Cancer*, **9**, 95-107.
 14. Eilers, M. and Eisenman, R.N. (2008) Myc's broad reach. *Genes Dev*, **22**, 2755-2766.
 15. Karin, M. (2006) NF-kappaB and cancer: mechanisms and targets. *Mol Carcinog*, **45**, 355-361.
 16. Massague, J. (2008) TGF-beta in Cancer. *Cell*, **134**, 215-230.
 17. Xu, Y. and Pasche, B. (2007) TGF-beta signaling alterations and susceptibility to colorectal cancer. *Hum Mol Genet*, 16 Spec No 1, R14-20.
 18. Budunova, I.V., Perez, P., Vaden, V.R., Spiegelman, V.S., Slaga, T.J. and Jorcano, J.L. (1999) Increased expression of p50-NF-kappaB and constitutive activation of NF-kappaB transcription factors during mouse skin carcinogenesis. *Oncogene*, **18**, 7423-7431.
 19. Kaur, J., Sharma, M., Sharma, P.D. and Bansal, M.P. (2008) Chemopreventive activity of lantadenes on two-stage carcinogenesis model in Swiss albino mice: AP-1 (c-jun), NFkappaB (p65) and P53 expression by ELISA and immunohistochemical localization. *Mol Cell Biochem*, **314**, 1-8.
 20. Van Hogerlinden, M., Rozell, B.L., Ahrlund-Richter, L. and Toftgard, R. (1999) Squamous cell carcinomas and increased apoptosis in skin with inhibited Rel/nuclear factor-kappaB signaling. *Cancer Res*, **59**, 3299-3303.
 21. Tang, X., Liu, D., Shishodia, S., Ozburn, N., Behrens, C., Lee, J.J., Hong, W.K., Aggarwal, B.B. and Wistuba, II (2006) Nuclear factor-kappaB (NF-kappaB) is frequently expressed in lung cancer and preneoplastic lesions. *Cancer*, **107**, 2637-2646.
 22. Sato, M., Shames, D.S., Gazdar, A.F. and Minna, J.D. (2007) A translational view of

- the molecular pathogenesis of lung cancer. *J Thorac Oncol*, **2**, 327-343.
23. Fogt, F., Zhuang, Z., Poremba, C., Dockhorn-Dworniczak, B. and Vortmeyer, A. (1998) Comparison of p53 immunoexpression with allelic loss of p53 in ulcerative colitis-associated dysplasia and carcinoma. *Oncol Rep*, **5**, 477-480.
 24. Harpaz, N., Peck, A.L., Yin, J., Fiel, I., Hontanosas, M., Tong, T.R., Laurin, J.N., Abraham, J.M., Greenwald, B.D. and Meltzer, S.J. (1994) p53 protein expression in ulcerative colitis-associated colorectal dysplasia and carcinoma. *Hum Pathol*, **25**, 1069-1074.
 25. Lashner, B.A., Shapiro, B.D., Husain, A. and Goldblum, J.R. (1999) Evaluation of the usefulness of testing for p53 mutations in colorectal cancer surveillance for ulcerative colitis. *Am J Gastroenterol*, **94**, 456-462.
 26. Guda, K., Giardina, C., Nambiar, P., Cui, H. and Rosenberg, D.W. (2001) Aberrant transforming growth factor-beta signaling in azoxymethane-induced mouse colon tumors. *Mol Carcinog*, **31**, 204-213.
 27. Takahashi, M. and Wakabayashi, K. (2004) Gene mutations and altered gene expression in azoxymethane-induced colon carcinogenesis in rodents. *Cancer Sci*, **95**, 475-480.
 28. Han, J.M., Myung, H. and Kim, S. (2009) Antitumor activity and pharmacokinetic properties of ARS-interacting multi-functional protein 1 (AIMP1/p43), *Cancer Letter*, in press.
 29. Kim, K.J., Park, M.C., Choi, S.J., Oh, Y.S., Choi, E.C., Cho, H.J., Kim, M.H., Kim, S.H., Kim, D.W., Kim, S. and Kang, B.S. (2008) Determination of three-dimensional structure and residues of the novel tumor suppressor AIMP3/p18 required for the interaction with ATM. *J Biol Chem*, **283**, 14032-14040.
 30. Park, S.G., Kang, Y.S., Ahn, Y.H., Lee, S.H., Kim, K.R., Kim, K.W., Koh, G.Y., Ko,

- Y.G. and Kim, S. (2002) Dose-dependent biphasic activity of tRNA synthetase-associating factor, p43, in angiogenesis. *J Biol Chem*, **277**, 45243-45248.
31. Lee, S.W., Kang, Y.S. and Kim, S. (2006) Multi-functional proteins in tumorigenesis: Aminoacyl-tRNA synthetases and translational components. *Current Proteomics*, **3**, 233-247.

Figure Legends

Fig.1. Apoptotic and p53 responses to DNA damage between the cells with different AIMP2 genotypes. (A) MEFs were exposed to UV (50J/m²) and apoptotic cells were determined by measuring sub-G1 portion (%) using flow cytometry. (**: P< 0.01) (B) Cell death was induced by the treatment of BPDE (0.1μM) and viable cells were counted in two day interval (2 dishes from each group). (C) Cells were harvested in 2 h after UV exposure. p53 (FL-393), phosphorylated p53 (ser 15), p21 and AIMP2 levels were determined by Western blotting. Tubulin was used as loading control.

Fig.2. TNF-α-dependent cell death and NF-κB induction (A) TNF-α induced cell death was determined by sub-G1 cells (%) as above. (**: P<0.01) (B) The plasmid encoding NF-κB-dependent luciferase was transfected into MEFs and incubated for 24 h. TNF-α was then treated for 12 h and luciferase activity was measured as described in methods. (*: P<0.05) (C) Cells were treated with murine TNF-α (30ng/ml) and the changes of IκB level was determined by Western blotting at the indicated times.

Fig.3. Differential sensitivity to growth arresting signal of TGF-β (A) Cell proliferation was monitored by the incorporation of radioactive thymidine. The percent inhibition of growth after the treatment of TGF-β was determined as described in methods. (**: P<0.01) (B) The effect of TGF-β on the expression of c-MYC was determined by quantitative real time RT-PCR. RNAs were isolated from the cells in 24 h after TGF-β treatment. Experiments were conducted in duplicates. (C) The effect of c-MYC on its target gene expression was monitored by cyclin D1-dependent luciferase activity. Cells were harvested in 12 h after

TGF- β treatment. (D) MEFs were grown in absence and presence of TGF- β . The cells of each group were cultivated in 6 dishes and 2 dishes were harvested at the indicated times and the cells were counted. (E) Schematic representation of AIMP2 activities in different signal pathways. It mediates pro-apoptotic response to DNA damage via p53 [6] and to TNF- α signal via TRAF2 [7]. It also enhances growth inhibition in TGF- β signaling through downregulation of c-MYC [8].

Fig.4. Differential susceptibility to chemical-induced skin papilloma (A) AIMP2 level was determined in AIMP2^{+/+} and AIMP2^{+/-} mouse skins by western blot (B and C) AIMP2 wild type and heterozygous mice were subjected to two stage skin carcinogenesis model using DMBA and TPA as described in methods and the numbers of papilloma on shaved back were counted at the indicated times. (D) Representative pictures showing skin papilloma formed on the back skin of the mice. (E) Papillomas were obtained and histology was observed by hematoxylin and eosin staining. Bar, 0.4 mm. (F) Paraffinized papillomas were subjected to TUNNEL assay. Apoptotic signal and nuclei are shown in green and red fluorescence, respectively. (magnification; \times 400) (G) The papilloma tissues were also subjected to immunohistochemistry with antibodies against PCNA (FL-261) and cyclinD1 (H-295) which are known proliferation markers. (magnification; \times 400).

Fig. 5. Differential responses to BP-induced lung carcinogenesis (A) AIMP2 levels in lung of AIMP2^{+/+} and AIMP^{+/-} mice were determined by western blot. (B) Lungs were isolated from mouse at indicated time interval and tumor nodules were counted. (C) Histological examination of the isolated lungs with tumors by hematoxylin and eosin staining. Bar, 40 μ m.

Fig.6. Differential responses to colon carcinogenesis (A) AIMP2 level in colon tissues of AIMP2^{+/+} and AIMP2^{+/-} mice were compared by western blot. (B) Polyps were induced by AOM and DSS as described in Methods. Colon regions were isolated from AIMP2^{+/+} and AIMP2^{+/-} mice and the number of polyp was counted. (*: P<0.05) (C) The representative polyps formed in the wild type and heterozygous mice are shown. Bar, 1mm.

Fig.1

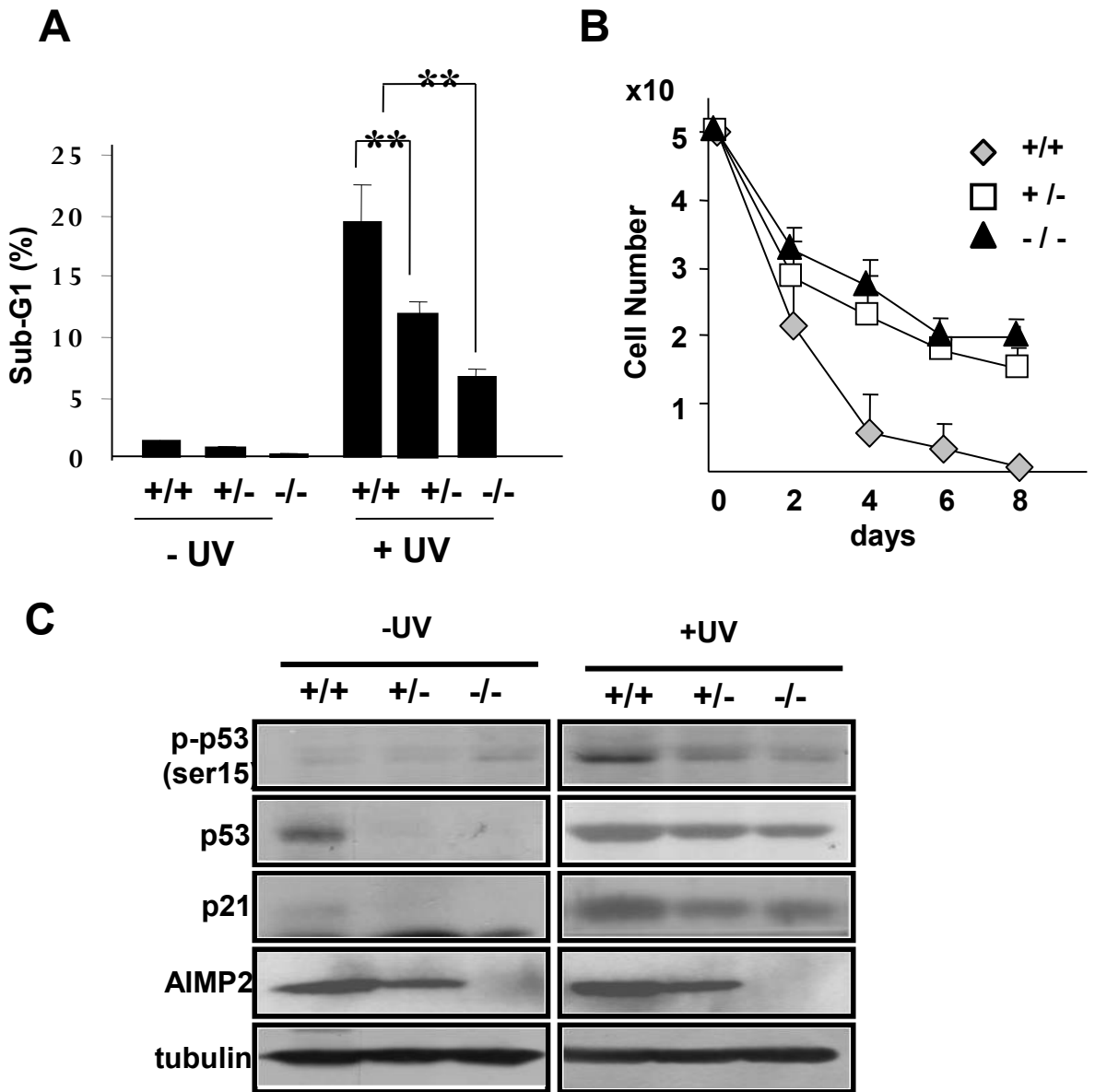


Fig.3

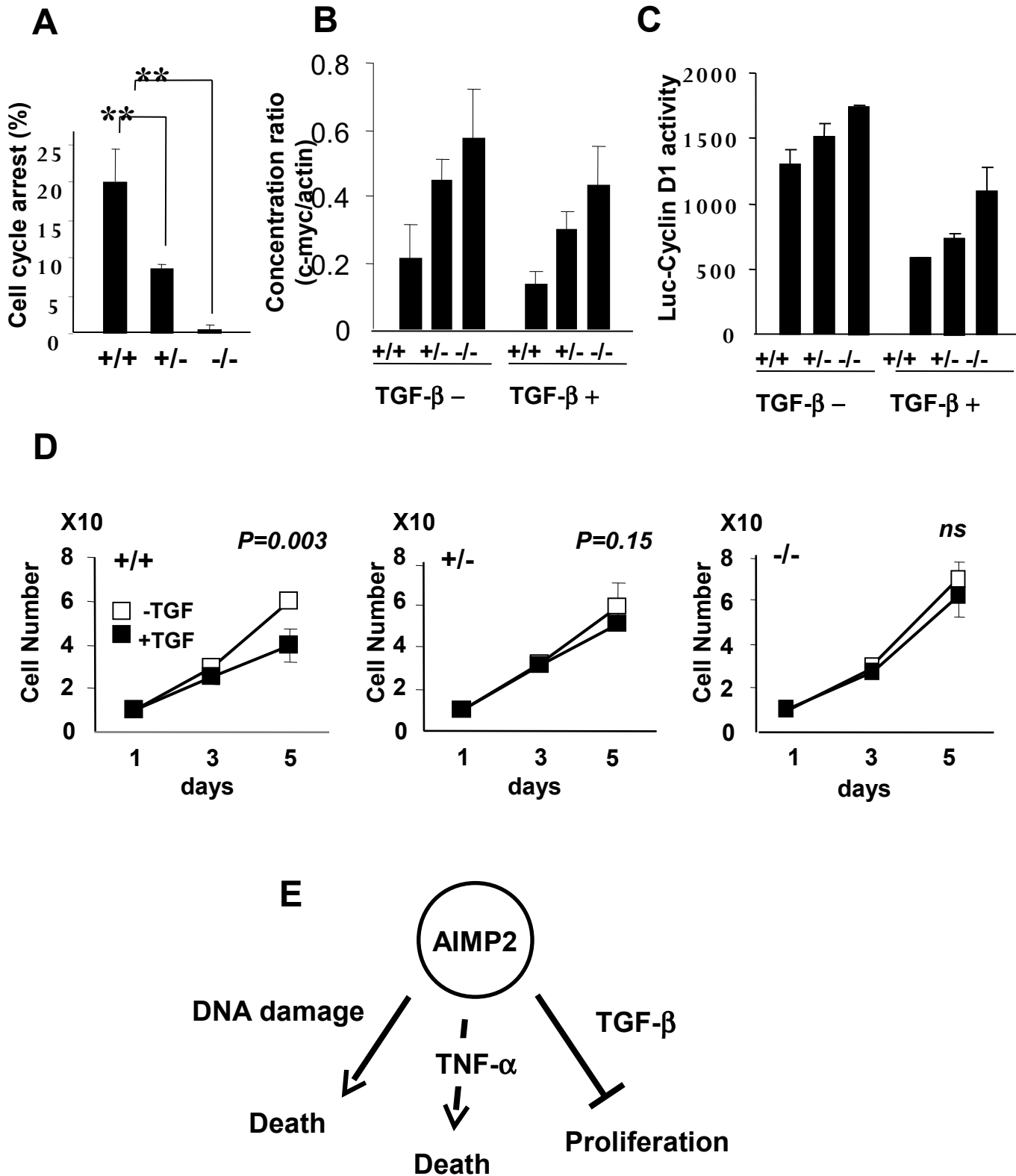


Fig.4

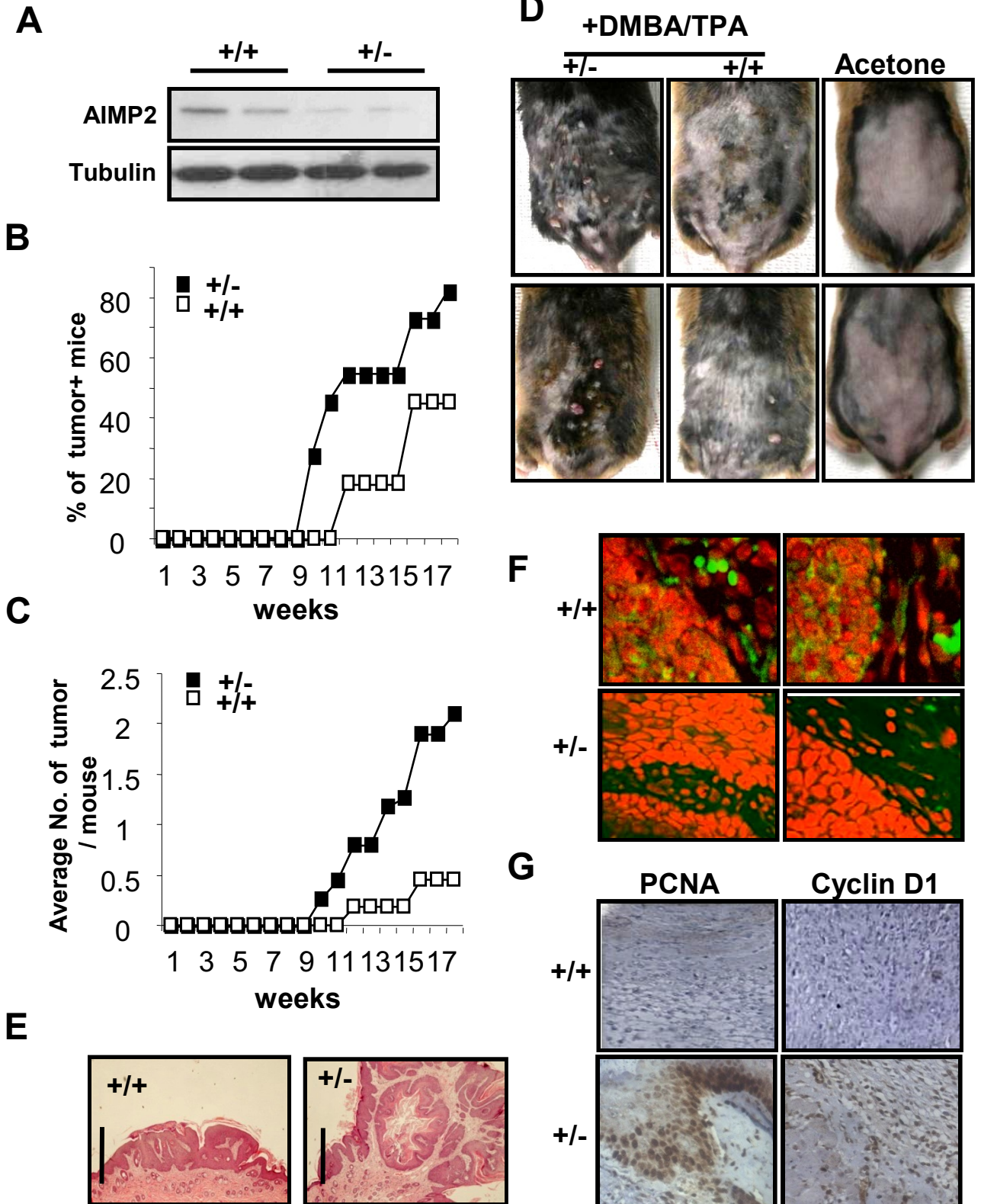


Fig.5

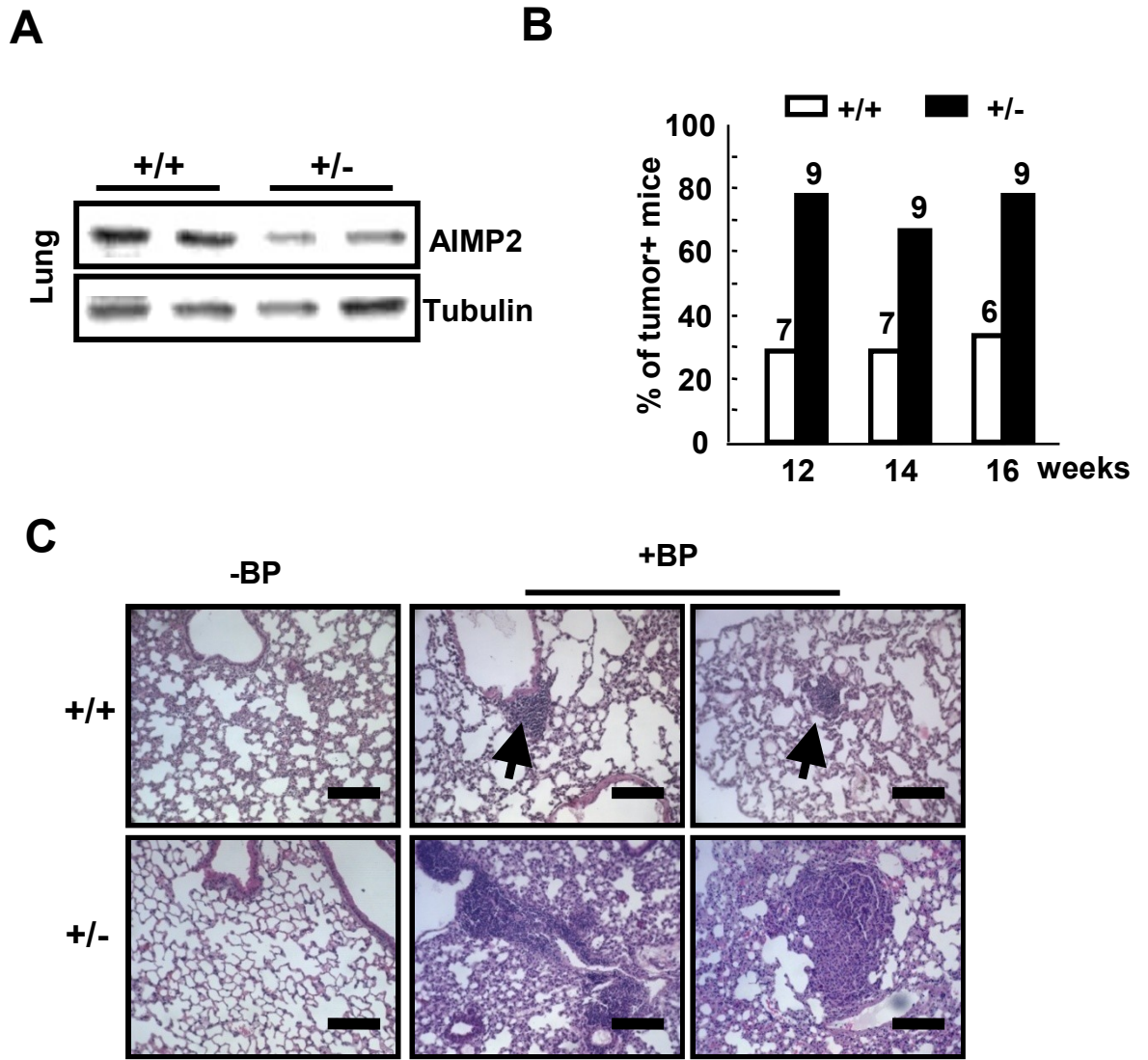


Fig.6

